

## RESEARCH ARTICLE

10.1002/2016JG003444

## Key Points:

- The effects of land use changes and other environmental changes on NEP were separated using a modified BIOME-BGC model
- Land use changes during 1985–2010 reduced NEP by more than 20%
- Increasing CO<sub>2</sub> concentration and nitrogen deposition compensated for a half of the total carbon loss

## Correspondence to:

X. Xu,  
xbxu@niglas.ac.cn

## Citation:


Xu, X., G. Yang, Y. Tan, X. Tang, H. Jiang, X. Sun, Q. Zhuang, and H. Li (2017), Impacts of land use changes on net ecosystem production in the Taihu Lake Basin of China from 1985 to 2010, *J. Geophys. Res. Biogeosci.*, 122, doi:10.1002/2016JG003444.

Received 6 APR 2016

Accepted 6 MAR 2017

All rights reserved. Article published online 9 MAR 2017

## Impacts of land use changes on net ecosystem production in the Taihu Lake Basin of China from 1985 to 2010

Xibao Xu<sup>1,2</sup> , Guishan Yang<sup>1</sup>, Yan Tan<sup>3</sup>, Xuguang Tang<sup>1</sup> , Hong Jiang<sup>4</sup>, Xiaoxiang Sun<sup>1</sup>, Qianlai Zhuang<sup>2</sup> , and Hengpeng Li<sup>1</sup>

<sup>1</sup>Key Laboratory of Watershed Geographic Sciences, Nanjing Institute of Geography and Limnology, Chinese Academy of Sciences, Nanjing, China, <sup>2</sup>Department of Earth, Atmospheric, and Planetary Sciences, Purdue University, West Lafayette, Indiana, USA, <sup>3</sup>Department of Geography, Environment and Population, University of Adelaide, Adelaide, South Australia, Australia, <sup>4</sup>School of Forestry and Bio-technology, Zhejiang A & F University, Lin'an, China

**Abstract** Land use changes play a major role in determining sources and sinks of carbon at regional and global scales. This study employs a modified Global biome model-biogeochemical cycle model to examine the changes in the spatiotemporal pattern of net ecosystem production (NEP) in the Taihu Lake Basin of China during 1985–2010 and the extent to which land use change impacted NEP. The model is calibrated with observed NEP at three flux sites for three dominant land use types in the basin including cropland, evergreen needleleaf forest, and mixed forest. Two simulations are conducted to distinguish the net effects of land use change and increasing atmospheric concentrations of CO<sub>2</sub> and nitrogen deposition on NEP. The study estimates that NEP in the basin decreased by 9.8% (1.57 Tg C) from 1985 to 2010, showing an overall downward trend. The NEP distribution exhibits an apparent spatial heterogeneity at the municipal level. Land use changes during 1985–2010 reduced the regional NEP (3.21 Tg C in year 2010) by 19.9% compared to its 1985 level, while the increasing atmospheric CO<sub>2</sub> concentrations and nitrogen deposition compensated for a half of the total carbon loss. Critical measures for regulating rapid urban expansion and population growth and reinforcing environment protection programs are recommended to increase the regional carbon sink.

### 1. Introduction

The Fifth Assessment Report of the *Intergovernmental Panel on Climate Change (IPCC)* [2014] asserts that anthropogenic greenhouse gas emissions have warmed the Earth's climate and climate change will have an increasing impact on natural and human systems in the next decades. Fossil fuel use and land use changes are two primary drivers to growing atmospheric CO<sub>2</sub> concentrations [Houghton *et al.*, 1999]. In particular, changes in land use and management have played a large part in determining sources and sinks of carbon, contributing to more than a third of the world's carbon emissions during 1850–2006 (330 Pg C; 1 Pg = 10<sup>15</sup> g) [Houghton, 2007]. Methodologically, integrating ecological models with remote sensing data has been developed in the last two decades, and over 40 sophisticated ecological models have been constructed to simulate the spatial and temporal patterns of carbon cycles of terrestrial ecosystems. Fundamental models include the Terrestrial Ecosystem Model (TEM) [Melillo *et al.*, 1993], CENTURY [Parton *et al.*, 1993], Carnegie-Ames-Stanford approach (CASA) [Potter *et al.*, 1993], Global biome model-biogeochemical cycle (BIOME-BGC) [Running and Hunt, 1993], and Boreal Ecosystems Productivity Simulator (BEPS) [Liu *et al.*, 1997]. Empirically, these ecological models have been widely applied: first, to estimate the spatial and temporal patterns of regional and global carbon cycles [Chiesi *et al.*, 2007; Houghton, 2007; Kicklighter *et al.*, 1999; Potter *et al.*, 1993; Schimel *et al.*, 2001] and, second, to disentangle the complex relationship between land use change, climate change, and carbon cycles of terrestrial ecosystems [McGuire *et al.*, 2001; Tatarinov *et al.*, 2011; Thornton *et al.*, 2002]. Increased understandings of carbon sinks and sources as well as the mechanisms of carbon cycling have not only lifted public awareness to climate change, but also fostered the development of theoretical frameworks and operational tools for policymakers to formulate policies on carbon mitigation and ecosystem conservation.

However, applying ecological models to examine the effect of land use changes on carbon cycling, a focus of this paper, faces at least four major challenges [Houghton, 2007; McGuire *et al.*, 2001]. First, scientific understanding of the characteristics of, and mechanisms for, net ecosystem production (NEP) (NEP = GPP – total respiration) for urban ecosystems remains limited, and thus, suitable models that can be applied to

estimate the NEP of urban ecosystems are scarce. High complexity and spatial heterogeneity of urban ecosystems and a limited number of eddy flux towers for urban ecosystems have further aggravated this problem [Crawford *et al.*, 2011; Ward *et al.*, 2015; Weissert *et al.*, 2014]. There is a knowledge gap in understanding the effect of land use change from nonurban land to urban land on the regional NEP. Second, many parameters of ecological models are difficult to regionalize due to their complexity and high sensitivity. Limited available data of flux observations exacerbates this challenge [Tang *et al.*, 2015b; Trusilova *et al.*, 2009; White *et al.*, 2000]. Third, the environmental factors which influence terrestrial ecosystems are still inadequately studied due to large regional disparities among terrestrial ecosystems [Gonzalez *et al.*, 2007; Kicklighter *et al.*, 1999]. Fourth, how to separate the distinct effects of land use changes from other environmental changes including CO<sub>2</sub> fertilization, N deposition, and climate change on carbon cycling presents an enormous challenge [Houghton, 2013; Houghton *et al.*, 1999; Jain *et al.*, 2013; McGuire *et al.*, 2001]. As outlined by Houghton [2013], separating the two effects can reduce the uncertainty of the land use change flux, help us understand a constellation of factors influencing terrestrial carbon balance, and explore the mechanisms (metabolic versus structural) in a consistent manner. However, the major challenge to separate these two effects is the lack of observations for testing flux estimates as a result of land use change alone. These challenges, methodological in nature, can create considerable uncertainties when applying ecological models and remote sensing data to estimate regional and global carbon balances. This study focuses on dealing with the second and fourth challenges by integrating ecological modeling, flux observation, and remote sensing data.

The Taihu Lake Basin (TLB), a core part of China's Yangtze River Delta, has experienced remarkable economic development since the mid-1980s, at an annual growth rate of 15.7% in gross domestic product (GDP), 3.0% in population growth, and 9.2% in urbanization. Rapid industrialization and urbanization has dramatically changed land use and land cover patterns and intensified the degradation risk of ecosystem services in the basin [Xu *et al.*, 2016]. As a result, land use change has significantly influenced regional carbon sequestration capacity, which has, in turn, constrained economic development in the region [IPCC, 2014; Schulp *et al.*, 2008]. Much work has been done on the following: carbon exchange mechanisms for agroecosystems [Ma *et al.*, 2013; Zhang *et al.*, 2014], greenhouse gas flux monitoring in the Taihu Lake [Lee *et al.*, 2014], soil carbon pool change in the agroecosystems [Pan *et al.*, 2008], land use optimization based on terrestrial ecosystem carbon storage [Chuai *et al.*, 2014], and the spatiotemporal distribution of net primary production (NPP) using the CASA model and Moderate Resolution Imaging Spectroradiometer (MODIS)/SPOT normalized difference vegetation index data [Wu *et al.*, 2014; Xu *et al.*, 2011]. Yet there remains a knowledge gap in quantifying the magnitude of NEP and in analyzing dynamics and drivers of the changing spatiotemporal pattern of carbon sequestration function in the basin. Moreover, the State Council of China has posited the establishment of "ecological red lines," a baseline that the country must strictly maintain to regenerate or improve ecosystem functions [Xinhuanet, 2013]. However, how the red lines can be defined is not clear. There is a pressing need to understand the changes of NEP, as it is a vital indicator to define the ecological red lines that distinguish the main ecological functional areas from economic development areas.

This study seeks to analyze how changes in nonurban land have impacted NEP and the spatiotemporal patterns of NEP in the TLB in 1985–2010. The analysis is based on our modified BIOME-BGC model and land use data for three periods derived from Landsat TM images. Using observed NEP from three flux sites, built on the open-path eddy covariance technique, we recalibrated fundamental parameters of the BIOME-BGC model for three dominant land use or land cover types in the basin: cropland, evergreen needleleaf forest, and mixed forest. Fossil fuel use was not considered in this study as our interest focused on how land use changes influenced NEP of terrestrial ecosystems. The study contributes to refining a set of suitable ecophysiological parameters by advancing simulation methods for NEP, reducing NEP uncertainty, partitioning the specific impacts of land use changes, increasing atmospheric concentrations of CO<sub>2</sub> and nitrogen (N) deposition on NEP, and suggesting adaptive countermeasures in the study area.

## 2. Methods

### 2.1. Study Region and Site Description

The TLB, situated on the east coast of China (within E119°3'1"–121°54'26", N30°7'19"–32°14'56"), encompasses one municipality (Shanghai) and most of two provinces of Jiangsu and Zhejiang (Figure 1). The basin

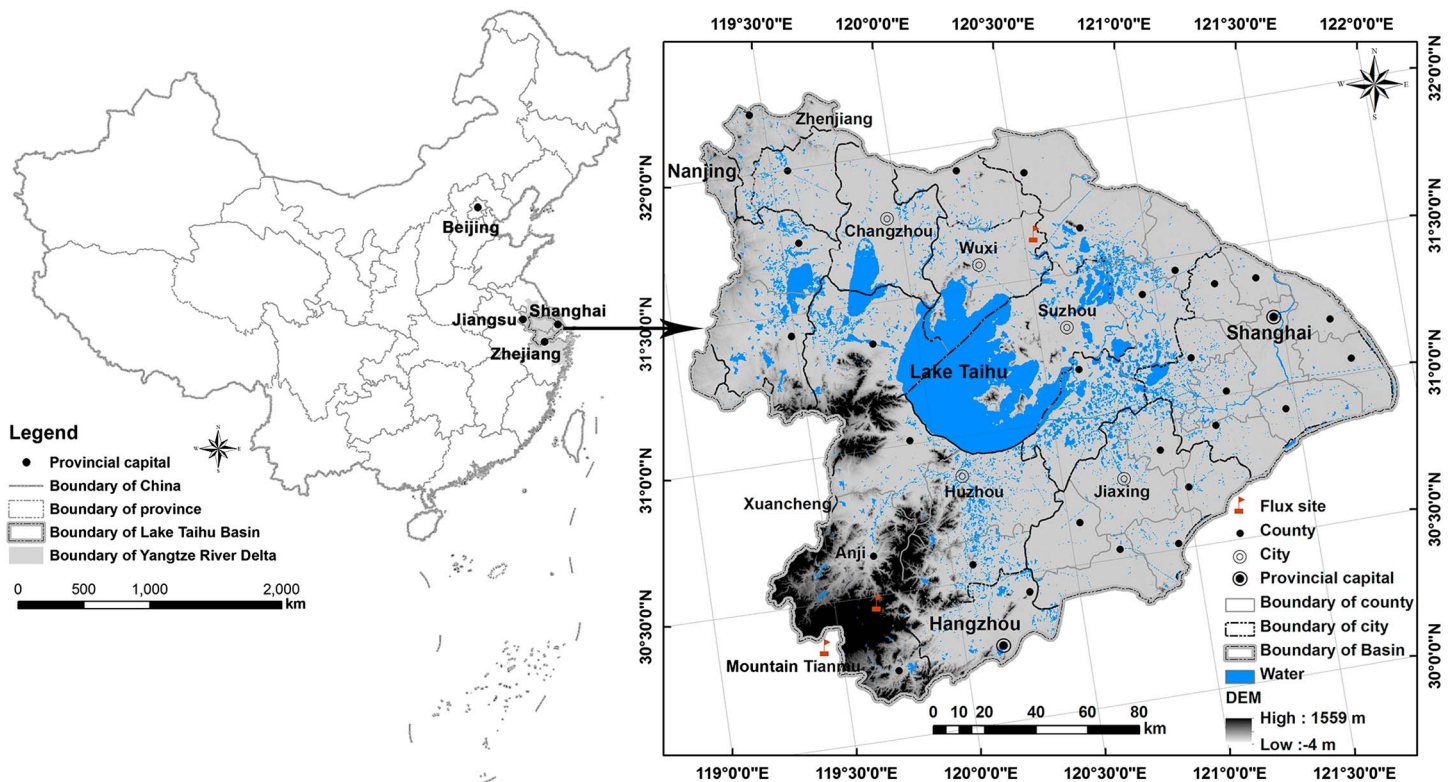


**Figure 1.** Location of the Taihu Lake Basin.

has a typical subtropical monsoon climate, with an annual mean temperature of 15–17°C and annual mean precipitation of 1010–1400 mm. Its average elevation is 34.4 m, varying between  $-4$  m and 1559 m. The dominant soil types are yellow brown soil, red soil, and paddy soil (agricultural land). Cropland, urban and builtup land, and water bodies make up 47.9%, 24.3%, and 13.6% of the total area of the basin, respectively, as reflected in our estimations derived from Landsat images in 2010. Among some 200 water bodies within the catchment, Taihu Lake is the largest and the third largest freshwater lake in China. Notably, the basin is one of the most populous and developed regions of China, accounting for 0.38% of China's total land area, supports 4.8% of the nation's 1.34 billion population, and produces 11.6% of the national gross domestic product (GDP) (USD 6471.2 billion, USD 1 = 6.41 yuan as of 25 August 2014). During the past 25 years the urban built area grew substantially (by 2.5 times the 1985 level). The basin encompasses China's largest urban cluster that involves 10 major cities (including Shanghai) in the region. Conversion of agricultural land to urban use is a major driver imposing significant effects on carbon sequestration. According to China's National New-Style Urbanization Plan (2014–2020), urbanization in this basin will be accelerated [*The State Council of the People's Republic of China*, 2014]. Sustained rapid urbanization in the region will undoubtedly lead to growing demand for land resources and cause further impact on carbon balance if urbanization and climate policies do not strictly regulate rapid land use change or if policies are implemented poorly in the coming years.

Three open-path eddy covariance towers were established for three dominant land use or land cover types including cropland, evergreen needleleaf forest, and mixed forest to observe net ecosystem  $\text{CO}_2$  exchange (NEE) ( $\text{NEP} = -\text{NEE}$ ) in the region (see Figure 1). Cropland (a system rotating between planting wheat in winter and rice in summer) accounted for 47.9% of total basin area (17,799.4  $\text{km}^2$ ), while evergreen needleleaf forest (ENF) and mixed forest accounted for 56.2% and 11.7% of the total forest area (5204.9  $\text{km}^2$ ) in 2010, respectively. In the land cover data sets over the 1985–2010 period, Moso bamboo, a dominant species, was classified as evergreen needleleaf forest (ENF) and accounted for 61.2% of the total area of ENF in 2010. Furthermore, the spatial distribution of Moso bamboo cannot be distinguished from other ENFs based on Landsat TM imageries. Thus, observed NEP and other parameters for Moso bamboo were used to represent all ENF in the model estimations. We acknowledge that this will lead to certainties in our estimated regional NEP. Future high-resolution land cover data that are able to separate Moso bamboo from other

evergreen needleleaf forests shall constrain the uncertainty. The flux site for Moso bamboo is located in Anji county (N30°28'34.5", E119°40'25.7"; elevation of 380 m above the sea; began in January 2011), and an LI7500 CO<sub>2</sub>/H<sub>2</sub>O analyzer (LI-COR, Inc., Lincoln, USA) and CSAT3 3-D sonic anemometer (Campbell Sci. Inc., USA) are set up there. Flux sites for cropland and mixed forest are located in Wuxi City (N31°39'14", E120°32'43"; elevation of 6 m above the sea; began in December 2011) and Mountain Tianmu (N30°20'59", E119°26'13"; elevation of 1140 m above the sea; began in January 2013). These two field sites are equipped with EC150 CO<sub>2</sub>/H<sub>2</sub>O analyzer (Campbell Sci. Inc., USA) and CSAT3 3-D sonic anemometers (Campbell Sci. Inc., USA).

## 2.2. Data Sources

Historical data sets include remote sensing images, meteorological data, and ancillary geospatial data. Land use data were interpreted from Landsat TM images in 1985, 2000, 2005, and 2010 at the scale of 1:100,000 based on a decision tree method. Land use data in 2010, which can be accessed through the Lake and Watershed Data Center (<http://lwdc.niglas.cas.cn>), were verified with some 2000 field samples, and the overall accuracy was above 90%. Land cover data in 1985 and 2005 at the scale of 1:250,000 were derived from Landsat TM images and MODIS images based on the land use data in 1985 and 2005 at the scale of 1:100,000, respectively. The satellite imagery sources were shared with the Data Sharing Infrastructure of Earth System Science, Chinese Academy of Sciences (CAS). Land use changes during 1985–2010 were derived from overlapping land use data of 1985 and 2010. The land use data sets of 1985–2010 were classified into five categories including cropland, forest, grassland, water, and urban and builtup. In the short term, specific types within the broad category of forest are not easy to change, but conversions from forest to other land use types (e.g., cropland and urban) usually occur. To meet the requirements for estimating the impact of land use change on NEP with high accuracy, forest data (1985, 2000, and 2010) were assimilated and classified into six subcategories (at much higher resolutions) based on land use data sets of 1985–2010 and land cover data sets of 1985–2005, including evergreen needleleaf forest, evergreen broadleaf forest, deciduous needleleaf forest, deciduous broadleaf forest, mixed forest, and shrubland.

We collected NEP data from three flux sites, looking into cropland over a 2 year period (from January 2012 to December 2013), evergreen needleleaf forest over a 2 year period (from January to June 2012 and from January to November 2013), and mixed forest over a 1 year period (January–December 2013). Observed NEP was processed successively through spike removing, a rotation of coordinates, frequency compensation, and Webb-Pearman-Leuning corrections. Any missing data for a short period (up to 3–4 h) were filled by linear interpolation, while missing data for a relatively longer period (up to a few days) were filled using a neural network model based on micrometeorological data (i.e., temperature, solar radiation, wind speed, air pressure, and air humidity) and soil monitoring data (i.e. soil temperature, soil moisture, and soil conductivity at 10 cm in depth).

Daily meteorological data of precipitation, maximum, and minimum temperature from 1980 to 2013 were obtained from the National Meteorological Center (NMC) of China. Such data were collected from 22 field observing stations in the basin and its adjacent areas. Daily short-wave radiation ( $W m^{-2}$ ), vapor pressure deficit (Pa), average daytime temperature, and the length of the daytime periods across the 22 field observing stations were estimated by using the Mountain microclimate model (MT-CLIM) [Glassy and Running, 1994]. Then these seven meteorological variables were interpolated to the whole basin by using the inverse distance weighted interpolation method [Bartier and Keller, 1996]. Average daytime temperature, daily maximum, and minimum temperatures were further calibrated with the digital elevation model (DEM). Data of 1:250,000 administrative district maps, DEM, and soil data sets were used to extract the geographical location, elevation, soil depth, and texture for the field sites. All spatial data were projected with Albers Conical Equal Area and transformed into a binary format at a spatial resolution of 250 m.

## 2.3. BIOME-BGC Model

The BIOME-BGC model simulates three vital biogeochemical cycles at a daily time step, including the following: carbon, nitrogen, and water within an ecosystem across several compartments, including the leaf, root, stem, soil, and air, using physiological process relationships [Running and Hunt, 1993; Thornton et al., 2002; White et al., 2000]. It requires daily meteorological data, information on the broad environment (i.e., soil, vegetation, and site condition), and parameters measuring the ecophysiological characteristics of vegetation. The BIOME-BGC model was initially developed to simulate the dynamics of forest carbon and nitrogen pools over

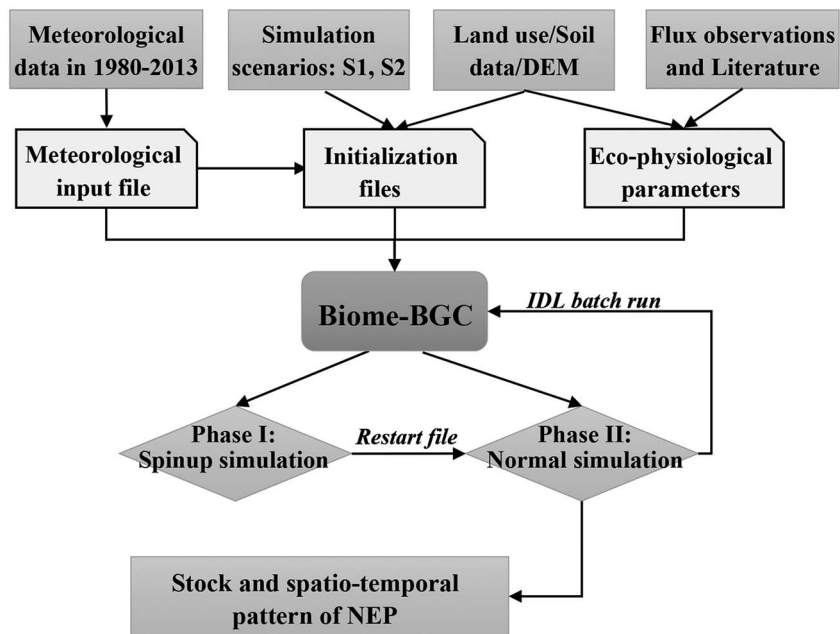


**Figure 2.** BIOME-BGC model: a simulation process for NEP on a regional scale.

time [Running and Hunt, 1993; White et al., 2000]. Recently, the BIOME-BGC model has been expanded to agricultural ecosystems such as winter wheat, corn, and paddy fields, where human activities such as irrigation, fertilizer application, and intensive cultivation influence the systems heavily [Hidy et al., 2012; Ma et al., 2013; Wang et al., 2005]. The studies of Wang et al. [2005] and Bai et al. [2014] suggested that the modified BIOME-BGC model can reasonably predict crop growth (leave area index (LAI) and net primary productivity (NPP)), evapotranspiration (ET), daily CO<sub>2</sub> and H<sub>2</sub>O fluxes of China’s agricultural ecosystems featured by the rotation between winter wheat and corn. Their modified BIOME-BGC model can take into account the effects of increasing atmospheric nitrogen and CO<sub>2</sub> concentrations and human management. To simulate managed herbaceous ecosystems, Hidy et al. [2012] modified a BIOME-BGC model which can accurately represent the effects of mowing and grazing. Ma et al. [2013] noted that an updated BIOME-BGC model (ANTHRO-BGC) was reliable to simulate the NEP, GPP, and ET of wheat, barley, and oilseed rape in Europe [Ma et al., 2013]. This model has been widely applied to local, regional, and global studies addressing carbon dynamics of different terrestrial ecosystems [Law et al., 2003; Wang et al., 2005], the effects of climate change and environmental disturbance [Han et al., 2014; Thornton et al., 2002], and the impact of land use change and management [Robinson et al., 2009; Robinson et al., 2013].

NEP represents the net accumulation or loss of carbon within an entire ecosystem. NEP can be defined as the difference between GPP and total respiration and estimated in the BIOME-BGC model as expressed in equation (1):

$$NEP = GPP - R_m - R_g - R_h \tag{1}$$

where GPP denotes gross primary production calculated using Farquhar’s photosynthesis routine [Farquhar et al., 1980];  $R_m$  denotes maintenance respiration from the leaves, stems, and roots, which is estimated as the function of tissue mass, nitrogen concentration, and temperature;  $R_g$  denotes growth respiration, which is simply estimated as a constant fraction of gross canopy photosynthetic rate minus maintenance respiration; and  $R_h$  denotes the respiration from litter and soil carbon pools, which is estimated using specified respiration rates at 15°C, the amount of carbon in these pools, a temperature dependent  $Q_{10}$  function [Kirschbaum, 1995], and a soil moisture-dependent factor [Running and Hunt, 1993; Thornton et al., 2002].

This study employs the latest version of the BIOME-BGC model and involves two phases (Figure 2). The first phase involves the spin-up run which brings the model into a steady state to estimate the initial soil carbon

and nitrogen [Thornton *et al.*, 2002; Wang *et al.*, 2009]. The second phase involves a normal transient simulation, which uses the initial carbon and nitrogen pools obtained from the first phase. The regional models usually have numerous parameters for various ecosystems (i.e., deciduous needleleaf, broadleaf forest, grassland, shrubland, and cropland). Their default values, however, must be modified for specific ecosystems as they respond to environmental conditions differently [Chiesi *et al.*, 2007; Tatarinov *et al.*, 2011; White *et al.*, 2000].

Stomatal conductance significantly influences the rate of flux of either water or carbon dioxide through the stomata [Trusilova *et al.*, 2009; White *et al.*, 2000]. The default stomatal conductance is not sensitive to the decrease in soil moisture content when it approaches the saturation point, but a small decrease in soil moisture can cause significant declines of stomatal conductance at lower soil moisture levels [Hidy *et al.*, 2012]. Located in the subtropical monsoon zone, soil moisture in our study area varies dramatically in summer due to frequent and huge shifts between dry and wet weather conditions. This variation can cause spikes in stomatal conductance. To avoid these spikes, this study applied the version 4.2 of BIOME-BGC with the modification of a relative soil moisture content suggested by Hidy *et al.* [2012].

The BIOME-BGC model contains a phenology module to simulate the exchanges of carbon dioxide and latent heat between the ecosystem and atmosphere for C<sub>3</sub> crops including rice and wheat [Hidy *et al.*, 2012; Wang *et al.*, 2005]. The phenological process is simulated by using prefixed dates for the start and end of the growing season for each crop. However, the rotation of crops (winter-wheat and summer-rice rotation) in an annual cycle cannot be simulated consecutively. Thus, the model structure was modified by adding a flag (1 for the wheat growing season and 0 for the rice growing season) into the `epc_file` block of the `Initialization_file` for the cropland. This flag was used to choose corresponding ecophysiological parameters according to the rotational season of wheat and rice, to simulate the consecutive daily NEP of the cropland on a yearly basis. The fixed dates for the start and the end point of the wheat- and rice-growing seasons in the corresponding `epc_files` were derived from the eddy covariance-based flux data (NEP is positive) and field observations (on the harvest day), respectively. Meanwhile, the prefixed dates for the start and the end point of the wheat- and rice-growing seasons may introduce discrepancies between simulations and actual observations due to interannual variability [Hidy *et al.*, 2012; Wu *et al.*, 2012], usually varying between 7 and 14 days in the study area.

Fertilization and irrigation are normal practices in utilizing cropland in the basin. The timing for fertilizing and irrigating and the amount of fertilizer used each time were recorded at our selected field observing sites. Such information was also added into the `Initialization_file`. As there was no historical record of these three parameters, the observation data in 2012 is used as initial approximation for the time span from 1980 to 2013. We note that this assumption may cause uncertainty as the amount of fertilizer and timing of fertilizer application vary significantly overtime [Wu *et al.*, 2012]. Meanwhile, although there is an alternative exchange between irrigation and soil drying during the rice-growing period, our observation data on soil moisture at depths 10 cm, 20 cm, and 40 cm during 2012–2013 were obtained at almost the saturated state. Soil moisture during the rice-growing season in the region was set to its saturated state (i.e. irrigation stopped 15 days before harvest) because water is not a constraint for rice growing in the basin due to adequate rainfall and convenient irrigation.

#### 2.4. Model Calibration and Validation

The BIOME-BGC model has 47 ecophysiological parameters. Before the calibration, built on existing studies [Hidy *et al.*, 2012; Ma *et al.*, 2011; White *et al.*, 2000], we conducted a sensitivity analysis to detect the most sensitive parameters of the model for wheat, rice, evergreen needleleaf forest, and mixed forest in the basin. NEP variation across these four different ecosystem types was sensitive to seven ecophysiological parameters including a transfer growth period as a fraction of a growing season, C:N of leaves, C:N of leaf litter, C:N of fine roots, canopy light extinction coefficient, maximum stomatal conductance, and boundary layer conductance. Moreover, the NEP of wheat and rice was sensitive to the prefixed dates for the start and the end point of the growing season. Literature shows that several sophisticated methods have been used to calibrate the BIOME-BGC model, including a linear regression analysis method [Trusilova *et al.*, 2009; Ueyama *et al.*, 2010; Wang *et al.*, 2005], Bayesian approach [Hidy *et al.*, 2012], nonlinear inversion [Ma *et al.*, 2011], and Monte Carlo experiments [Petritsch *et al.*, 2007]. In the present study we applied Monte Carlo and linear regression analysis methods to evaluate and optimize the BIOME-BGC model.

**Table 1.** Ecophysiological Parameters for Key Types of Ecosystems in the Taihu Lake Basin

Parameters	Wheat	Rice	Evergreen Needleleaf	
			Forest (ENF)	Mixed Forest
Year day to start new growth	50 <sup>a</sup>	171 <sup>a</sup>	0 <sup>c</sup>	0 <sup>c</sup>
Year day to end litterfall	151 <sup>a</sup>	304 <sup>a</sup>	0 <sup>c</sup>	0 <sup>c</sup>
Transfer growth period as fraction of growing season	0.55	0.65	0.25	0.25
C:N of leaves	65 <sup>a</sup>	35 <sup>a</sup>	22.1 <sup>b</sup>	27
C:N of leaf litter	85 <sup>a</sup>	65 <sup>a</sup>	55 <sup>b</sup>	65
C:N of fine roots	120 <sup>a</sup>	85 <sup>a</sup>	60 <sup>b</sup>	42
Canopy light extinction coefficient	0.48	0.48	0.6	0.7
Maximum stomatal conductance	0.006	0.006	0.006	0.006
Boundary layer conductance	0.003	0.003	0.01	0.01
leaf water potential: complete conductance reduction	−4.7	−4.7	−4.3	4.3

<sup>a</sup>Coefficients observed at the flux sites.

<sup>b</sup>Coefficients suggested by other relevant studies [Hou, 2010; B. Z. Zhou, 2006; G. M. Zhou, 2006].

<sup>c</sup>"0" indicated as the flag to drive the phenology submodel to simulate "year day to start new growth" and "year day to end litterfall". For ENF, its growing and litterfall seasons complete in a year. For the mixed forest, new growth begins if the length of the daytime period is over 10 h and 55 min (39,300 s) or the running sum of the daily mean soil temperature (Tavg) (when the average soil temperature is above 0°C) is above a critical value ( $\exp(4.795 + 0.129 * Tavg)$ ). Litterfall begins if the length of daytime period is less than 39,300 s and the soil temperature is lower than the mean soil temperature in fall (September and October) or if the soil temperature drops below 2°C. Litterfall stops when 50% of all live fine roots and leaves are removed.

Daily cropland NEP in 2012 (December 2011 to November 2012), daily NEP of Moso bamboo in 2011 and daily NEP of mixed forest in 2013 were used to calibrate model parameters for these three ecosystem types. Daily NEP of cropland in 2013, daily NEP of Moso bamboo in 2012 (January–May) and daily NEP of mixed forest in 2014 (January–May) were used to validate the model. We used an ensemble Monte Carlo simulation method to calibrate the BIOME-BGC model by altering ecophysiological parameters with  $\pm 1\%$  intervals and assessing the goodness of fit between measured and modeled NEP values on daily and monthly scales with  $R^2$  value, respectively. Parameter values for the prefixed dates for the start and the end point of the growing season, C: N of leaves, C:N of leaf litter, and C:N of fine roots for wheat and rice were derived from our field observations at the flux sites. Additional four sensitive ecophysiological parameters were obtained from the calibration (Table 1). The validations were assessed with the goodness of fit between modeled and measured NEP using a linear regression.

As apparent in Figure 3 and Table 2, our calibrated BIOME-BGC models for cropland, evergreen needleleaf forest, and mixed forest have been improved significantly. At the daily scale, the  $R^2$  value in the annual NEP simulation models for cropland, evergreen needleleaf forest, and mixed forest was 0.59, 0.30, and 0.41, respectively. At the monthly scale, the  $R^2$  value of calibration was 0.85, 0.46, and 0.86, respectively. The  $R^2$  value of validation for cropland, evergreen needleleaf forest, and the mixed forest was 0.55, 0.31, and 0.45, respectively, at a daily scale; and that of validation for cropland was 0.86 at the monthly scale. These statistics suggest that the modified model, using actual flux observation data, has a robust capacity in predicting NEP on a regional scale. As the area of grassland accounts for only 0.34% of total area of the basin, and also because of a lack of NEE flux data for grassland in this study, we used the default parameters for grassland with no calibration. Also, the default parameter settings for evergreen/deciduous broadleaf forest, deciduous needleleaf forest, shrubland, and grassland in the original model were simply applied to our study due to the unavailability of local observation data. As shown in Figures 3 and 4, the simulated NEP during the wheat overwintering period (from December to early February in the following year) in both the calibration and validation models was underestimated because this period was predefined as a nongrowing season. Another underestimation appeared in summer months (July–August 2013) because of high-temperature stress (with a daily mean temperature of 32.8°C) on carbon sequestration during the rice-growing season (Figure 4). There were 59 days with the daily mean temperature hitting over 30° in Wuxi in 2013. Furthermore, there was a notable underestimation of NEP for the needleleaf forest in summer (July–August 2011) (Figure 3). This underestimation of NEP was primarily due to two factors. The first one is high by water stress because of prolonged hot weather. Rainfall was reduced by 505 mm in July–August 2011, which was much less than the usual amount over the 2 month period in normal years. There were

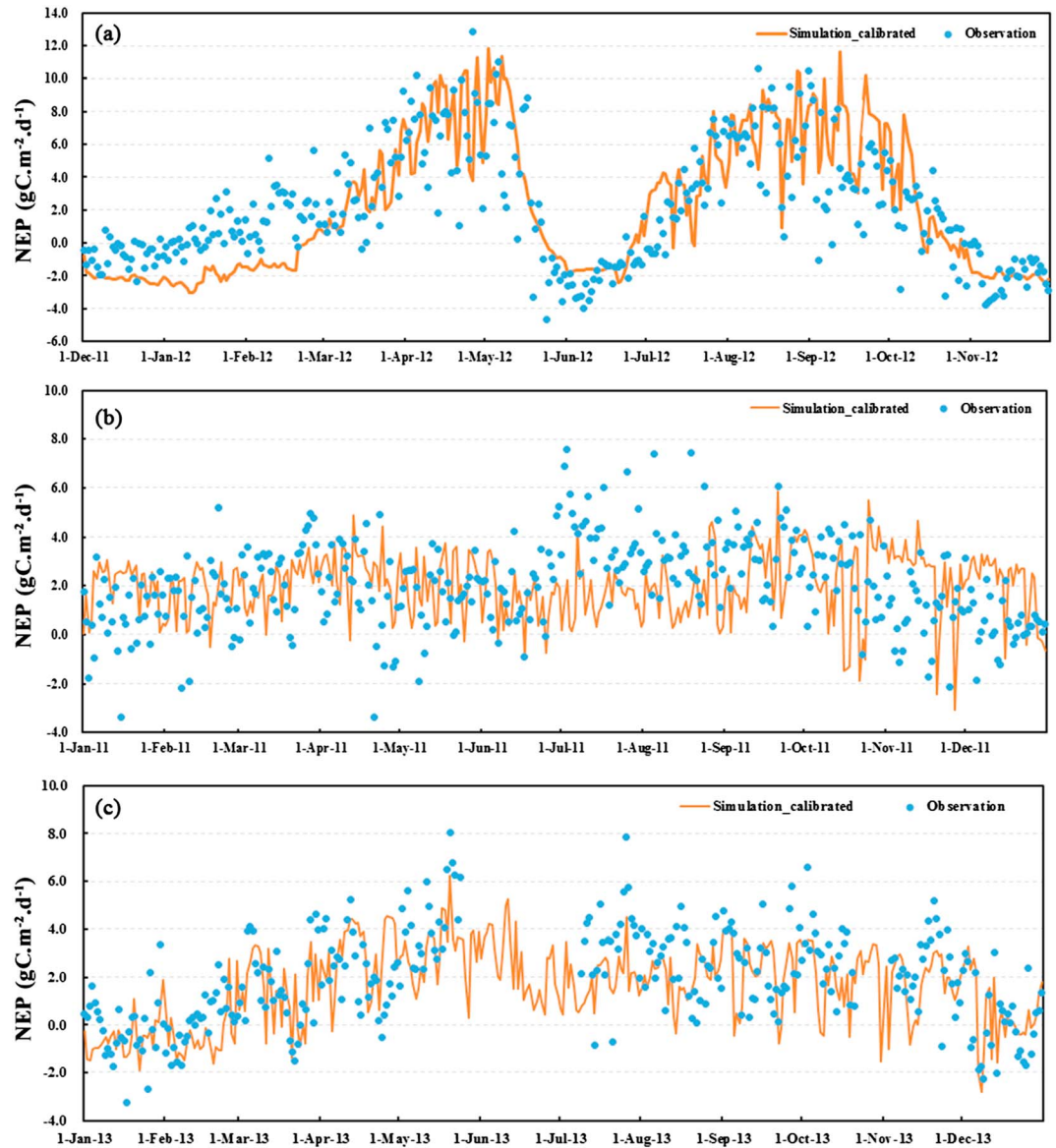


**Figure 3.** Comparison between the observed and simulated daily NEP based on the calibrated BIOME-BGC models for: (a) cropland, (b) evergreen needleleaf forest, and (c) mixed forest.

**Table 2.** Model Performance Statistics of the Calibration and Validation<sup>a</sup>

Model Performance Statistics	Cropland		ENF		MF	
	Daily	Monthly	Daily	Monthly	Daily	Monthly
<i>Calibration</i>						
$R^2$	0.59	0.85	0.30	0.46	0.41	0.86
NRMSE: Normalized root-mean-square error	0.15	0.18	0.20	0.21	0.14	0.14
RAD: relative average deviation (%)	16.5	17.2	19.5	16.9	21.6	10.8
<i>Validation</i>						
$R^2$	0.55	0.86	0.31	0.45	0.45	0.84
NRMSE: Normalized root-mean-square error	0.17	0.15	0.32	0.40	0.15	0.24
RAD: relative average deviation (%)	17.6	17.9	37.8	35.2	12.0	14.6

<sup>a</sup>Note:  $NRMSE = RMSE / (X_{obs,max} - X_{obs,min})$ .  $X_{obs,max}$  and  $X_{obs,min}$  are monthly/daily observed maximum and minimum values, respectively, with units of  $g\ C\ month^{-1}$  or  $g\ C\ d^{-1}$ . NRMSE is unitless.



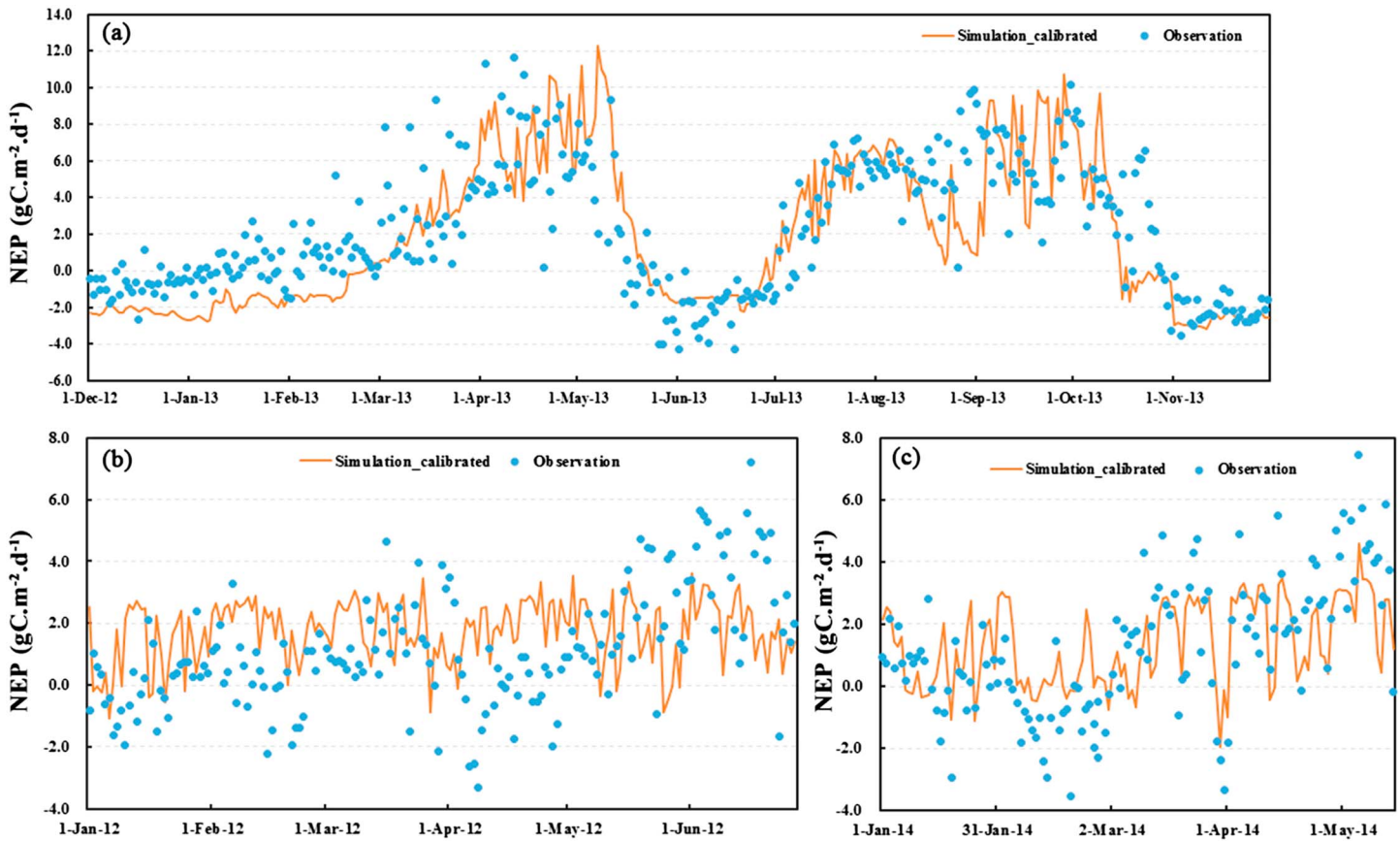
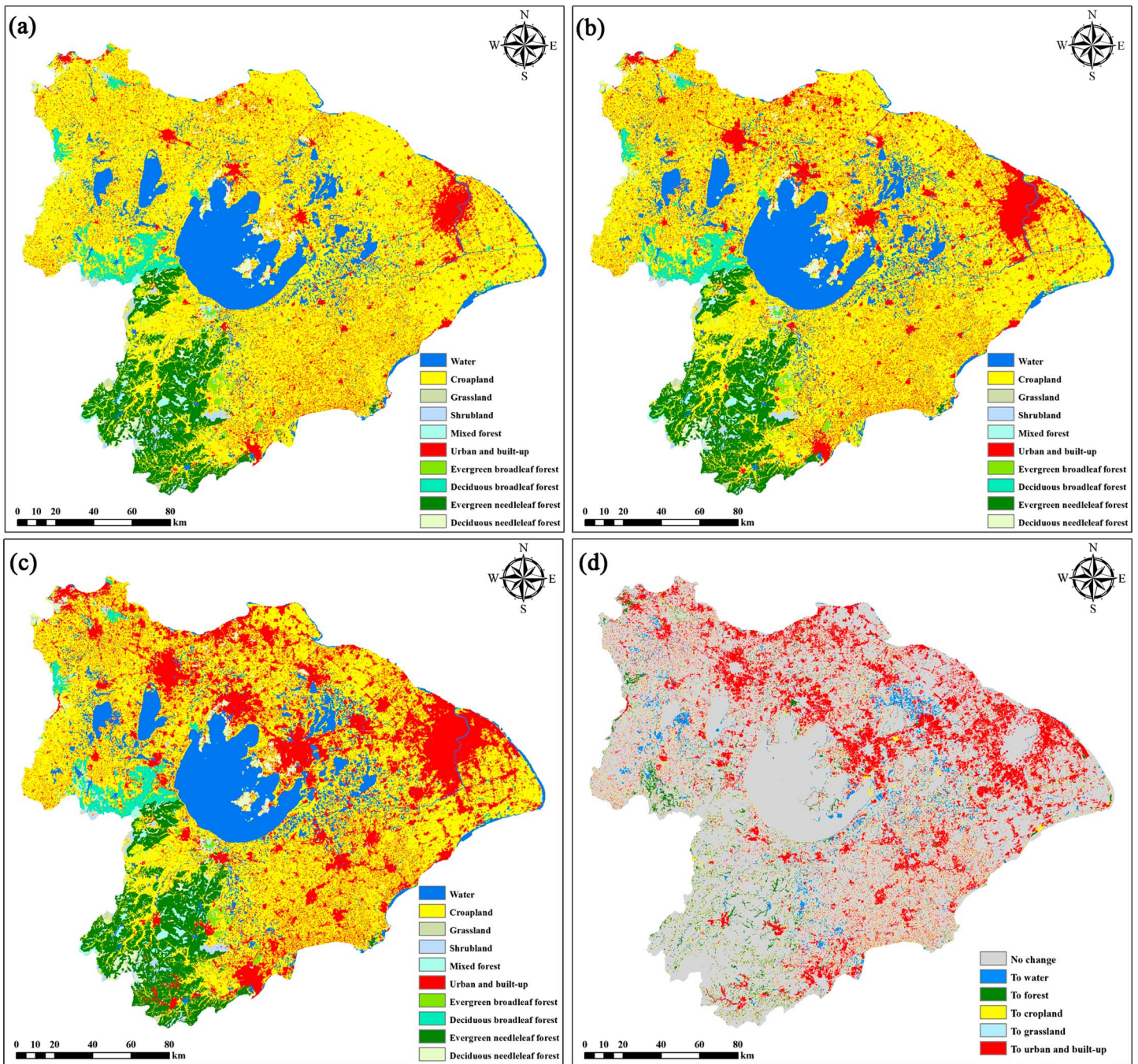


Figure 4. Validation between the observed and simulated daily NEP for (a) cropland, (b) evergreen needleleaf forest, and (c) mixed forest.

24 days with a daily mean temperature above  $30^{\circ}\text{C}$  in the region. Consequently, the water potential multiplier (ranging from 0.0 to 1.0), the lower values, and the higher water stress on GPP dropped quickly to lower than 0.3. While growth respiration, maintenance respiration, and heterotrophic respiration all remained at high level due to high temperature, which resulted in low NEP. Actually, bamboo has a deep and abundant root system, which can extract deep groundwater to maintain a water balance. As showed by *G. M. Zhou* [2006], the aboveground and underground carbon storage accounted for 32.8% and 67.2% of the total carbon storage of bamboo ecosystems, respectively. However, our simulations estimated the aboveground and soil carbon pool accounting for 83.0% and only 17.0% of the total carbon pool, respectively. These could be two main reasons why the goodness of fit for bamboo was lower than that of cropland and mixed forest. Future BIOME-BGC development shall consider the deep-water effects on bamboo carbon dynamics.

### 2.5. Model Simulation

To estimate the distinct effects of land use change and increasing atmospheric concentration of  $\text{CO}_2$  and N deposition on carbon sequestration, we conducted model simulations under two situations. The first situation (S1) deals with the actual outcomes of NEP under the interactions between land use change and increasing atmospheric concentration of  $\text{CO}_2$  and N deposition. As shown in earlier data collected by the Mauna Loa Observatory, Hawaii (1980–2013), annual atmospheric  $\text{CO}_2$  concentration increased from 338.32 ppm in 1980 to 395.31 ppm in 2013. Accordingly, in our study atmospheric N deposition was initialized according to the temporal trajectory of  $\text{CO}_2$  mole fraction, based on two reference rates of  $0.0005 \text{ kg m}^{-2}$  in 1985 and  $0.0021 \text{ kg m}^{-2}$  in 2000 to scale N deposition levels to  $\text{CO}_2$  concentration levels [*Liu et al.*, 2013; *Wang et al.*, 2005]. The second situation (S2) assumes that atmospheric  $\text{CO}_2$  concentration and N deposition remain unchanged at their 1985 levels: 338.32 ppm and  $0.0005 \text{ kg m}^{-2}$ , respectively. To smoothen the effect of



**Figure 5.** Changes in land use and land cover in the Taihu Lake Basin, 1985–2010. (a) Land use in 1985, (b) land use in 2000, (c) land use in 2010, and (d) land use change in 1985–2010. Color bar in Figure 5d represents land use types in 2010 converted from other types of land use in 1985.

volatile meteorological conditions on NEP, an average annual NEP over 7 year intervals (1982–1988, 1997–2003, and 2007–2013, respectively) is used as the simulated NEP for years of 1985, 2000, and 2010, to reflect land use patterns over these three time periods. For those areas without change in land use/land cover since 1985, the simulations, using the same ecological parameters, proceed throughout all years from 1985 to 2010. Otherwise, the simulation process would stop when it approaches to a specific year (i.e. 2000, 2005, and 2010) during which land use/land cover changed. In such circumstances the models respin-up using the corresponding ecological parameters for a new land use type and then continue to proceed normal simulations.

**Table 3.** Matrix of Land Use Conversion (Km<sup>2</sup>) in the Taihu Lake Basin During 1985–2010

Land use types in 1985	Land Use Type in 2010													
	Cropland	Urban and Built-Up	Water	Evergreen Needleleaf Forest		Evergreen Broadleaf Forest		Deciduous Needleleaf Forest		Deciduous Broadleaf Forest		Mixed Forest	Shrubland	Grassland
				Forest	Forest	Forest	Forest	Forest	Forest	Forest	Forest			
Cropland	16246.3	5938.3	846.3	226.6	32.1	45.1	70.2	224.1	13.2	0.8				
Urban and built-up	764.6	2766.4	40.8	8.4	3.6	11.0	3.1	10.6	0.7	0.9				
Water	445.9	161.9	4101.3	5.4	0.6	6.0	3.6	17.6	0.6	3.3				
Evergreen needleleaf forest	144.6	34.3	9.9	2666.7	0.4	0.1	0.0	17.1	0.3	0.5				
Evergreen broadleaf forest	22.0	14.6	4.1	0.9	181.2	0.0	0.0	5.1	0.6	0.5				
Deciduous needleleaf forest	24.6	44.8	7.1	3.8	0.0	482.6	0.0	5.4	0.2	0.0				
Deciduous broadleaf forest	51.2	21.0	4.4	0.0	0.0	0.0	579.9	12.0	0.0	0.0				
Mixed forest	85.6	26.4	20.1	12.5	1.7	2.8	1.6	313.7	1.6	2.0				
Shrubland	11.9	4.9	0.3	0.1	0.3	0.0	0.0	1.3	226.1	0.0				
Grassland	2.9	5.8	8.1	0.3	0.3	0.3	1.9	0.3	1.6	105.8				

In the spin-up process, the number of spin-up years depends on the climate and vegetation characteristics, but it should not exceed the maximum number of spin-up years. In this study, the maximum number of spin-up years was set with 6000 based on the calibrations. The spin-up run stops when the difference between the annual mean and daily soil carbon stocks is less than a specified spin-up tolerance value (0.0005 kg m<sup>-2</sup> yr<sup>-1</sup>). Meteorological data across 34 years (1980–2013) are used to execute the spin-up runs to establish the steady state values for the soil carbon and nitrogen pools and to derive related restart files. Then the normal simulation is run successively.

The regional NEP is equal to the sum of the product of the NEP of nonurban land times the fractional area of nonurban land and the product of the NEP of urban land times the fractional area of urban land. Due to the high complexity and spatial heterogeneity of urban ecosystems in the basin, only NEP from urban forest was considered in this study, while NEP from energy use by other sectors such as urban transportation, households, and buildings was not considered. As urban forest cannot be precisely separated from urban built-up land use, the NEP for urban built-up areas was set to be constant, at the mean value (16.64 gC m<sup>-2</sup> yr<sup>-1</sup>) of carbon sequestration for urban forests across the cities of Nanjing, Shanghai, Hangzhou, Wuxi, and Taizhou in the region [Chen, 2015; Shi, 2013]. This mean value was estimated by the annual carbon sequestration of urban forest against the total area of urban built-up for each city. In addition, due to the lack of flux data for rivers/lakes, the NEP for rivers/lakes was constantly set with the monitored mean value (7.35 gC m<sup>-2</sup> yr<sup>-1</sup>) in the Taihu Lake from January 2003 to June 2005 by using a closed chamber technique [Ji et al., 2006]. The simulations on the regional scale were manipulated with a batch file derived from an interactive data language software.

### 3. Results

#### 3.1. Land Use and Land Cover Changes

Rapid economic and population growth in 1985–2010 has dramatically changed land use and land cover in the basin (Figure 5 and Table 2) [Xu et al., 2016]. This change was characterized by fast expansion of urban land areas. The urban land area increased by 1.5 times in 2010 compared to 1985 at the cost of a massive loss of cropland (5843.6 km<sup>2</sup>, or 24.7% of the 1985 level). The water body and forest increased marginally, by 296.3 km<sup>2</sup> (6.2%) and 138.9 km<sup>2</sup> (2.7%), respectively. The increase in water body was associated with two factors. First, the cultivated area within a 5 km radius of the Taihu Lake was returned to water body under the national “Returning Cropland to

**Table 4.** Estimated Changes in Annual Total NEP ( $\text{Gg C yr}^{-1}$ ,  $1 \text{ Gg C} = 10^9 \text{ g C}$ ) Under Two Situations During 1985–2010

Land Use Type	1985		2000		2010	
	S1	S2	S1	S2	S1	S2
Cropland	14,033.7	13,591.4	14,046.6	12,532.6	12,015.9	10,250.6
Forest						
Evergreen needleleaf	1,608.4	1,376.3	1,763.8	1,400.1	1,827.6	1,406.0
Evergreen broadleaf	36.7	27.1	43.3	26.4	41.2	26.0
Deciduous needleleaf	99.8	74.8	111.9	74.1	113.4	72.6
Deciduous broadleaf	86.5	39.0	103.8	38.1	109.4	38.5
Mixed forest	111.6	72.6	135.3	70.3	198.4	89.8
Shrubland	42.7	34.9	48.8	35.4	47.8	35.1
Grassland	1.9	12.6	2.8	9.8	1.4	9.7
Urban and built-up	60.1	60.1	83.0	83.0	150.1	150.1
Water	34.9	34.9	37.3	37.3	37.1	37.1
Total (TgC)	16.1	15.3	16.4	14.3	14.5	12.1

Lake” project implemented in the region since 2007. This project has been one of the key ecological projects to curb the deteriorating water quality of the Taihu Lake since the water crisis caused by algae blooms in 2007. Second, some of cropland has been converted to water body as the fishery industry brings farmers higher profit than grain cropping. Since 2007, China has implemented a fundamental land use policy under which  $120 \times 10^6$  ha of arable land are considered to be the minimum necessary to ensure its food security. A number of adaptive strategies for farmland exploitation, consolidation, and reclamation have been reinforced in the region since 2000. Consequently,  $764.6 \text{ km}^2$  of urban and built-up land,  $445.9 \text{ km}^2$  of water body, and  $339.9 \text{ km}^2$  of forest were converted to cropland over 1985–2010. Moreover, the national “Grain to Green” project (i.e., returning cropping land on steep slopes with a gradient of  $25^\circ$  or greater to forest or grassland) has been carried out since 2000, which has subsequently returned  $611.3 \text{ km}^2$  of cropland on steep slopes to forest in the region.

### 3.2. Regional NEP

The total NEP in the basin shows a persistent picture, decreasing by  $1.57 \text{ Tg C}$  (or 9.8%) under situation S1 and  $3.21 \text{ Tg C}$  (or 20.9%) under situation S2, from 1985 to 2010 (Table 3). Overwhelmingly, the NEP from cropland decreased by  $2.02 \text{ Tg C}$ , compared to some moderate increases from the forest (by  $0.35 \text{ Tg C}$ ), urban built-up (by  $0.09 \text{ Tg C}$ ), and water body (by  $0.002 \text{ Tg C}$ ). These increases in NEP were mainly associated with the increasing areas of forest, urban built-up, and water body, by  $138.9 \text{ km}^2$  (2.7%),  $5408.4 \text{ km}^2$  (149.8%), and  $296.3 \text{ km}^2$  (6.2%), respectively.

### 3.3. Spatial and Temporal Patterns of Change in NEP

At the city level, change in NEP exhibits an apparent spatial heterogeneity. Most of the major cities in the basin including Shanghai; Suzhou, Wuxi and Changzhou in Jiangsu province and Jiaxing and Hangzhou in Zhejiang province have witnessed enormous declines in NEP. Together, these cities contributed nearly three quarters (71.1%) to the total NEP of the basin in 2010 (Table 4). Enormous declines in NEP appear in the eastern and northern parts of the basin (Figures 6a and 6b). Strikingly, the megacity Shanghai and the three major cities (Suzhou, Wuxi, and Changzhou) of Jiangsu account for 98.5% of the total reduction of NEP in the basin (Table 4). In contrast, NEP presents a slight upward trend in Huzhou, and some parts of the cities of Xuancheng (Anhui province) and Nanjing (Jiangsu province) situated within the basin (Table 4). Change in NEP is significantly correlated with land use patterns and increased urban areas.

### 3.4. Impacts of Land Use Change and Increasing $\text{CO}_2$ Concentration and N Deposition on NEP

Through calculating the difference in NEP under two situations, the net effect of land use change (Figure 6b) and increasing  $\text{CO}_2$  concentration and N deposition on change in NEP (Figure 6c) can be identified. Except for grassland, water, urban, and built-up, each simulated mean NEP for the corresponding land use type under S1 is greater than that under S2 (Table 5). This result suggests that increasing atmospheric  $\text{CO}_2$  concentration and N deposition has positive effects on the carbon sequestration of the terrestrial ecosystems, contributing  $1.63 \text{ Tg C}$  to the NEP and thus compensating 50.9% of the total carbon loss induced by land use changes. It is worth noting that there may be some uncertainties in the NEP changes for evergreen broadleaf, deciduous

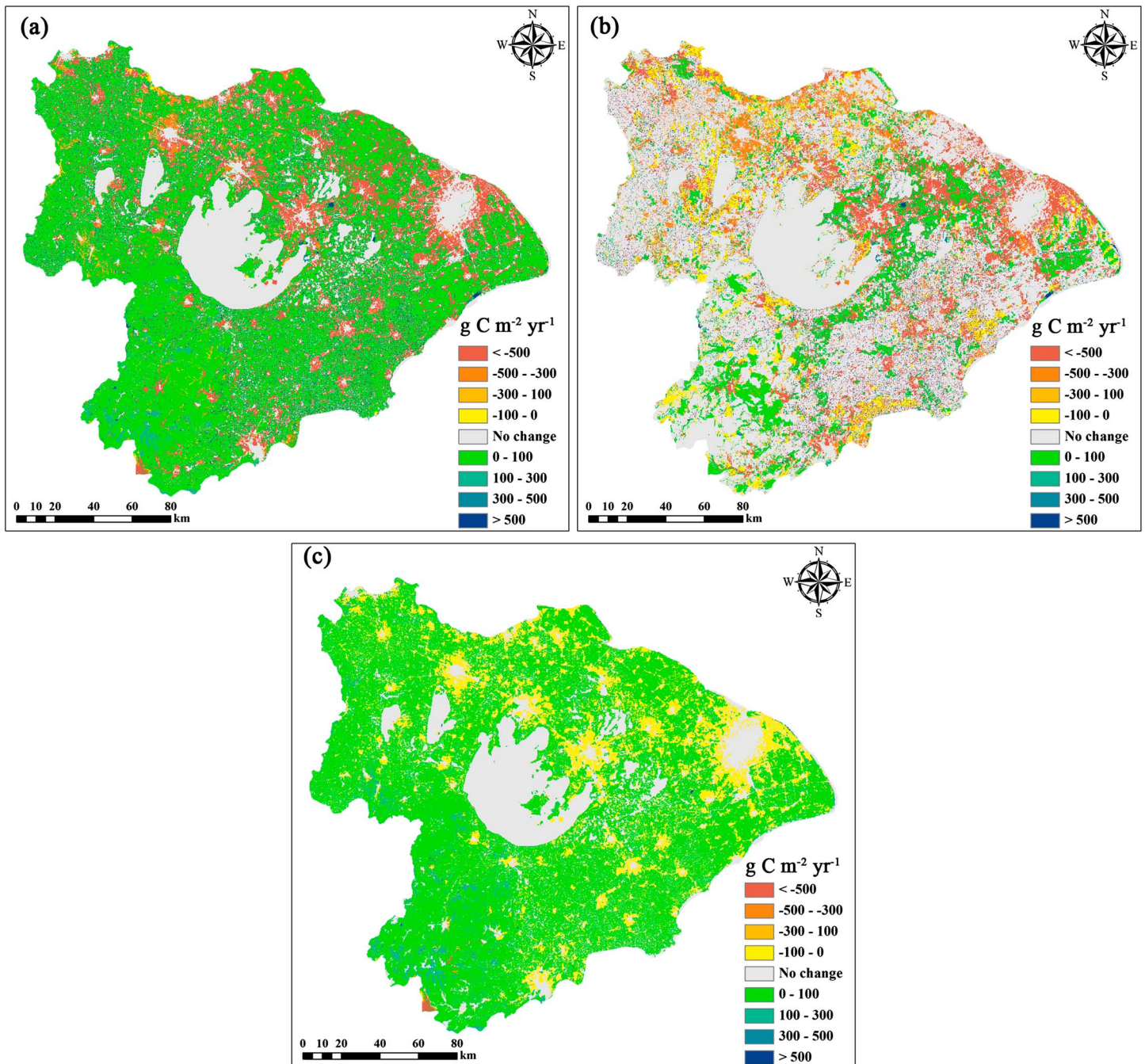


**Figure 6.** Simulated changes in NEP under two situations during 1985–2010: (a) from 1985 to 2010 under situation S1, (b) from 1985 to 2010 under situation S2, and (c) net changes in NEP caused by environmental changes of CO<sub>2</sub> fertilization and N deposition.

needleleaf, deciduous broadleaf, shrubland, and grassland, as there are no calibrations for these land use types (Table 6).

#### 4. Discussion

##### 4.1. Policy Implications

Dramatic urbanization and industrialization have resulted in significant land use change and subsequently caused tremendous loss of carbon sequestration in the Taihu Lake Basin since 1985. The trade-off between

**Table 5.** Changes in NEP, Land Use, Urban Areas, Population, and GDP, by City, 1985–2010<sup>a</sup>

City	NEP in 2010 (Tg C)	NEP Change (%)	Land Use Change (%)	Growth in Urban Area (%)	GDP Growth (%)	Population Growth (Times)
Suzhou	2.39	−20.8	26.5	259.5	112.8	19.2
Huzhou	3.04	6.1	17.2	102.7	51.8	11.6
Shanghai	1.84	−22.7	32.5	136.3	62.7	9.4
Wuxi	1.40	−14.7	25.6	182.0	71.6	19.3
Changzhou	1.62	−8.6	26.7	167.2	60.5	17.6
Jiaxing	1.73	−5.2	28.1	84.2	55.1	13.7
Hangzhou <sup>b</sup>	1.19	−3.4	23.7	117.2	66.3	34.1
Zhenjiang <sup>b</sup>	0.89	−8.4	26.6	141.7	58.3	10.3
Xuancheng <sup>b</sup>	0.10	14.7	15.4	2.8	n/a	n/a
Nanjing <sup>b</sup>	0.10	13.6	14.5	11.8	78.0	7.6

<sup>a</sup>Source: NEP based on BIOME-BGC model simulations. Land use change (%) and growth in urban areas (%) based on our land use and land cover data in 1985 and 2010. Growth in GDP and population based on statistical data of each city in 1985 and 2010.

<sup>b</sup>Only part of the city is located within the basin. Land use change (%) was measured as the proportion of the area for land use types converted from 1985 to 2010 in each city against the total area in each corresponding city.

economic and population growth and carbon emissions is, therefore, a fundamental issue of concern for policymakers and urban planners in this region [Xu *et al.*, 2016]. Based on the results of this study, three countermeasures are suggested as follows.

First, regulating accelerated urban sprawl and population growth. Land use changes during 1985–2010 have caused a total reduction in NEP by 3.10 Tg C in this basin. Cropland encroachment led to the largest reduction in NEP (by 3.34 Tg C) since cropland encroachment contributed 95% to urban sprawl during the 25 year period to 2010. One practical option to curtail further encroachment on cropland is to increase land use intensity in the urban areas. The Chinese government has designated urbanization as the “number one policy topic” since 2014, meaning that this policy will be a key determinant of the rate at which the encroachment process occurs in the next decade. A new-style urbanization approach to shifting from a conventional to a new model characterized by an intensive, smart, green, and low-carbon economy, and limiting massive inflows of rural migrants to the mega- and large-scale cities in the region is needed. In addition, the distinction between intermediate use and ultimate demand for cropland within the basin should be considered in population policymaking from both production and consumption perspectives [Chen and Han, 2015].

Second, reinforcing current environmental programs that protect cropland, forest, and wetland. As shown in Tables 2 and 3, the forest area increased by 138.9 km<sup>2</sup> (2.7%) and accordingly the related NEP increased by 41.2 GgC (2.7%) during 1985–2010. Moreover, average NEP for cropland, evergreen needleleaf forest and mixed forest increased from 593.6, 560.1, and 238.4 g C m<sup>−2</sup> a<sup>−1</sup> in 1985 to 675.1, 624.8, and 326.6 g C m<sup>−2</sup> a<sup>−1</sup>, respectively. Therefore, these programs, particularly the Grain to Green and Returning Cropland to Lake designated

**Table 6.** Simulated Changes in Annual Mean NEP (g C m<sup>−2</sup> yr<sup>−1</sup>) Under Two Situations

Land Use Type	1985		2000		2010	
	S1	S2	S1	S2	S1	S2
Cropland	593.6	574.9	640.5	571.5	675.1	575.8
Forest						
Evergreen needleleaf	560.1	479.2	605.4	480.6	624.8	480.7
Evergreen broadleaf	160.4	118.4	193.3	117.7	187.2	118.3
Deciduous needleleaf	175.6	131.7	200.2	132.6	207.0	132.7
Deciduous broadleaf	129.3	58.4	157.1	57.7	165.7	58.3
Mixed forest	238.4	155.7	285.7	148.5	326.6	148.1
Shrubland	174.3	142.4	197.4	143.1	195.4	143.6
Grassland	15.0	99.7	23.9	84.6	12.7	85.1
Urban and built-up	16.6	16.6	16.6	16.6	16.6	16.6
Water	7.4	7.4	7.4	7.4	7.4	7.4

to be completed in 2015 or 2020, should be extended to 2020 and beyond. Such programs have evidently played a vital role in improving carbon sink and other ecosystem services (e.g., water quantity adjustment, biodiversity, and water purification) and could continue to serve well into the future.

Third, using NEP, in combination with other measures of water quality, air pollution, and ecological conservation, as a primary indicator to define the “ecological red lines” [Chen *et al.*, 2009; Xu *et al.*, 2016]. NEP is a fundamental measure of the ecosystem function at the interface of varying risk landscapes related to climate change and carbon emissions and changing land use stimulated by urbanization and industrialization.

#### 4.2. Limitations and Future Work

This study improves the quantification of carbon cycles of cropland, evergreen needleleaf forest, and mixed forest ecosystems in the basin based on flux observations, remote sensing data, and a modified ecological model. A set of refined ecophysiological parameters of BIOME-BGC model was acquired. These parameters shall be applicable to other similar environments in China and other regions for quantifying ecosystem carbon dynamics. We find that the calibrated BIOME-BGC model, using our flux observations, simulated NEP with higher accuracy than existing studies which used a CASA model for this basin [Wu *et al.*, 2014; Xu *et al.*, 2011]. For example, our estimated average NEP of cropland ( $675.1 \text{ g C} \cdot \text{m}^{-2} \cdot \text{a}^{-1}$ ) is close to our observed NEP ( $767.4 \text{ g C} \cdot \text{m}^{-2} \cdot \text{a}^{-1}$ ) in this basin. The estimated average NEP of cropland is similar to the result ( $626.9 \text{ g C} \cdot \text{m}^{-2} \cdot \text{a}^{-1}$ ) as estimated by other researchers for the Huaihe River Basin, an area immediately adjacent to the Taihu Lake Basin [Li *et al.*, 2009; Xu *et al.*, 2015]. In contrast, using the CASA model, the estimated average NPP for this basin in an earlier study by Xu *et al.* [2011] was only  $666.5 \text{ g C m}^{-2} \text{ a}^{-1}$  in 2007, which was much lower than the estimated and observed values in this present study. However, four limitations to our modeling results deserve mention.

First, our estimated NEP for urban forests in urban areas ( $16.64 \text{ g C m}^{-2} \text{ yr}^{-1}$ ) and rivers/lakes ( $7.35 \text{ g C m}^{-2} \text{ yr}^{-1}$ ) could be too high due to likely underestimation of the impact of land use changes for these categories [Karim *et al.*, 2008; Xing *et al.*, 2005; Zhao *et al.*, 2010]. Available results from emerging studies [e.g., Chen, 2015; Weissert *et al.*, 2014] indicated that carbon stock and sequestration of urban trees varied considerably between, and within, cities and that urban vegetation cannot compensate for  $\text{CO}_2$  emissions on an annual basis in midlatitude cities due primarily to the small fraction of the area and low density of urban forest. Given the fact that urban areas and water bodies accounted for 38% of the total area of the basin in 2010, there is a great uncertainty in estimating regional NEP under this assumption. NEP of urban land and water bodies will need future research using  $\text{CO}_2$  fluxes and sophisticated models to identify their potential contributions to carbon mitigation. Also, for the purpose of carbon mitigation and its related policy-making, it will be helpful to assess regional carbon balance through incorporating carbon sequestration of terrestrial ecosystems and fossil fuel carbon emission in a future study.

Second, this study derived calibrated ecophysiological parameters from a few field observing sites to estimate NEP on a regional scale. This approach might introduce some uncertainties when scaling up the model. Some reliable remote sensing data on vegetation, such as MODIS products of leaf area index (LAI), gross primary production (GPP), and net primary production (NPP), can be further incorporated to calibrate the model [Zhu and Zhuang, 2014]. The observed water flux (evapotranspiration, ET) and latent heat flux (based on the eddy covariance technique) can also be included in the calibration [Tang *et al.*, 2015a; Trusilova *et al.*, 2009; Ueyama *et al.*, 2010]. The ecosystem flux data will help refine model parameters to quantify NEP more precisely on regional scale in the future.

Third, while the modified BIOME-BGC model approximately simulated NEP for  $\text{C}_3$  crops (wheat and rice), Moso bamboo and mixed forest in this study, the phenology module for the  $\text{C}_3$  crops and Moso bamboo needs to be further advanced. For example, the low sensitivity of fraction of leaf N in Rubisco for Moso bamboo is inconsistent with the study of White *et al.* [2000]. The possible reason could be the insufficient capacity of the phenology module in capturing the phenological process of Moso bamboo, especially during the rapid growing season of bamboo shoots from March to April in a year. The phenology module for the  $\text{C}_3$  crops and Moso bamboo could be improved by adopting dynamic start and end dates of the growing seasons which were estimated with the heat sum growing season index [Hidy *et al.*, 2012] or by using a new phenology module as constructed and tested by Ma *et al.* [2011]. In our study the modified BIOME-BGC model can effectively capture the dynamics of NEP for the cropland and relatively well capture the rotation between wheat and rice. However, the

changes of carbon inflows and outflows, carbon, and nutrient contents in the soil profile caused by wheat-rice rotation and changes in land conversion between cropland and forest on the NEP dynamics were not fully considered in the currently modified model [Bai *et al.*, 2014]. These will unavoidably lead to errors in our regional quantification. Further, BIOME-BGC model development shall incorporate the effects of crop rotation on soil carbon and nutrient dynamics like in the DeNitrification-DeComposition (DNDC) [Giltrap *et al.*, 2010] and Joint UK Land Environment Simulator (JULES) models [Clark *et al.*, 2011].

Finally, how to simulate the impacts of the conversion from croplands and other nonforest types to forests on the carbon cycle needs more research in the future. Many studies show that forest age significantly influences its carbon cycle [Boris *et al.*, 2010; Tomáš *et al.*, 2014]. A critical abstraction in the BIOME-BGC model is to ignore plant successional dynamics within its spatial context. Based on this abstraction, all the pools are dimensionless and can be regarded as buckets for storage rather than actual plant structures with known height, width, lengths, and age. Furthermore, flux observations from two towers for bamboo and mixed forests used in our model calibrations were from mature forests. The simulations for all forest types in this study were assumed to be steady state mature forests. This assumption may cause some underestimation of the impact of land use change on regional NEP, especially the impact of successional conversation. Thus, a longer time series of forest age data needs to be incorporated to further calibrate and refine the BIOME-BGC. Future research should also consider combining some empirical forest growth and yield models (e.g., European Forest Information Scenario model (EFISCEN) and Simulator of forest biodynamics (SIBYLA)) to increase accuracy of simulations of the forest carbon cycle [Boris *et al.*, 2010; Tomáš *et al.*, 2014].

## 5. Conclusion

This study refined and advanced the BIOME-BGC simulation approach, and subsequently used it to analyze the effects of land use changes and climate variation on NEP in the Taihu Lake Basin of China from 1985 to 2010. Model simulations found that the regional NEP of nonurban land declined by 9.8% (1.57 Tg C) during this period. Land use changes led to a total reduction in NEP by 3.21 Tg C (or 19.9% of the 1985 level), but the increasing atmospheric CO<sub>2</sub> concentration and N deposition compensated for a half of this reduction. Significant declines of NEP appeared in the rapidly urbanizing areas centered around mega and large cities in eastern and northern parts of the basin. Carbon emissions induced by land use change can be expected to maintain a growing momentum in the ongoing processes of urbanization and economic development in this basin in the next decade. The trade-offs between economic and population growth and carbon emissions should therefore be a compelling issue of concern for policymakers and urban planners in this region. Practical countermeasures including regulating accelerated urban sprawl and population growth in major metropolitan areas, and reinforcing environmental programs and afforestation programs were recommended.

### Acknowledgments

This study was supported by the National Natural Science Foundation of China (41371532, 41030745, and 41101565), the Interdisciplinary Frontier Project of Nanjing Institute of Geography and Limnology, CAS (NIGLAS2016QY02), the Australian Research Council Discovery project (DP110105522), a NASA Land-Use and Land-Cover Change project to Q.Z. (NASA-NNX09AI26G), and key project of CAS (KZZD-EW-10-04). We would like to express our great gratitude to Steve Running and Jared W. Oyster at the Numerical Terra Dynamic Simulation Group for helping run the model to the Data Sharing Infrastructure of Earth System Science, CAS, and the National Meteorological Center (NMC) of China for sharing data. Land use data set can be accessed through the Lake and Watershed Data Center (<http://lwdc.niglas.cas.cn>). Carbon flux and other auxiliary data can be obtained by contacting the corresponding author.

## References

- Bai, J., X. Chen, L. Li, G. Luo, and Q. Yu (2014), Quantifying the contributions of agricultural oasis expansion, management practices and climate change to net primary production and evapotranspiration in croplands in arid northwest China, *J. Arid. Environ.*, *100*, 31–41, doi:10.1016/j.jaridenv.2013.10.004.
- Bartier, P. M., and C. P. Keller (1996), Multivariate interpolation to incorporate thematic surface data using inverse distance weighting (IDW), *Comput. Geosci.*, *22*(7), 795–799.
- Boris, T., Z. Giuliana, J. V. Pieter, C. Galina, V. Nicolas, K. H. John, and L. Marcus (2010), A comparison of alternative modelling approaches to evaluate the European forest carbon fluxes, *For. Ecol. Manage.*, *260*, 241–251.
- Chen, G., and M. Han (2015), Global supply chain of arable land use: Production-based and consumption-based trade imbalance, *Land Use Policy*, *49*, 118–130, doi:10.1016/j.landusepol.2015.07.023.
- Chen, W. Y. (2015), The role of urban green infrastructure in offsetting carbon emissions in 35 major Chinese cities: A nationwide estimate, *Cities*, *44*, 112–120.
- Chen, Z., G. Chen, B. Chen, J. Zhou, Z. Yang, and Y. Zhou (2009), Net ecosystem services value of wetland: Environmental economic account, *Commun. Nonlinear Sci. Numer. Simul.*, *14*(6), 2837–2843, doi:10.1016/j.cnsns.2008.01.021.
- Chiesi, M., F. Maselli, M. Moriondo, L. Fibbi, M. Bindi, and S. W. Running (2007), Application of BIOME-BGC to simulate Mediterranean forest processes, *Ecol. Modell.*, *206*(1–2), 179–190, doi:10.1016/j.ecolmodel.2007.03.032.
- Chuai, X. W., X. J. Huang, W. J. Wang, C. Y. Wu, and R. Q. Zhao (2014), Spatial simulation of land use based on terrestrial ecosystem carbon storage in coastal Jiangsu, China, *Sci. Rep.*, *4*, 5667, doi:10.1038/Srep05667.
- Clark, D. B., et al. (2011), The Joint UK Land Environment Simulator (JULES), model description—Part 2: Carbon fluxes and vegetation dynamics, *Geosci. Model Dev.*, *4*(3), 701–722, doi:10.5194/gmd-4-701-2011.
- Crawford, B., C. S. B. Grimmond, and A. Christen (2011), Five years of carbon dioxide fluxes measurements in a highly vegetated suburban area, *Atmos. Environ.*, *45*(4), 896–905, doi:10.1016/j.atmosenv.2010.11.017.



- Farquhar, G. D., S. V. Caemmerer, and J. A. Berry (1980), A biochemical-model Of photosynthetic CO<sub>2</sub> assimilation in leaves Of C-3 species, *Planta*, 149(1), 78–90, doi:10.1007/Bf00386231.
- Glassy, J. M., and S. W. Running (1994), Validating diurnal climatology of the MT-CLIM model across a climatic gradient in Oregon, *Ecol. Appl.*, 4(2), 248–257.
- Giltrap, D. L., C. S. Li, and S. Saggar (2010), DNDC: A process-based model of greenhouse gas fluxes from agricultural soils, *Agric. Ecosyst. Environ.*, 136(3–4), 292–300, doi:10.1016/j.agee.2009.06.014.
- Gonzalez, O. R., C. Kuper, K. Jung, P. C. Naval, and E. Mendoza (2007), Parameter estimation using simulated annealing for S-system models of biochemical networks, *Bioinformatics*, 23(4), 480–486, doi:10.1093/bioinformatics/btl522.
- Han, Q. F., G. P. Luo, C. F. Li, and W. Q. Xu (2014), Modeling the grazing effect on dry grassland carbon cycling with BIOME-BGC model, *Ecol. Complex.*, 17, 149–157, doi:10.1016/j.ecocom.2013.12.002.
- Hidy, D., Z. Barcza, L. Haszpra, G. Churkina, K. Pinter, and Z. Nagy (2012), Development of the BIOME-BGC model for simulation of managed herbaceous ecosystems, *Ecol. Modell.*, 226, 99–119, doi:10.1016/j.ecolmodel.2011.11.008.
- Hou, X. J. (2010), Study on water characteristic in soil-plant-atmosphere continuum (SPAC) of *Phyllostachys pubescens* (in Chinese), Master's thesis, Beijing, China.
- Houghton, R. A. (2007), Balancing the global carbon budget, *Annu. Rev. Earth Planet. Sci.*, 35, 313–347, doi:10.1146/annurev.earth.35.031306.140057.
- Houghton, R. A. (2013), Keeping management effects separate from environmental effects in terrestrial carbon accounting, *Global Change Biol.*, 19(9), 2609–2612, doi:10.1111/gcb.12233.
- Houghton, R. A., J. L. Hackler, and K. T. Lawrence (1999), The US carbon budget: Contributions from land-use change, *Science*, 285(5427), 574–578, doi:10.1126/science.285.5427.574.
- Intergovernmental Panel on Climate Change (IPCC) (2014), *Climate Change 2014: Synthesis Report*, 151 pp., IPCC, Geneva, Switzerland.
- Jain, A. K., P. Meiyappan, Y. Song, and J. I. House (2013), CO<sub>2</sub> emissions from land-use change affected more by nitrogen cycle, than by the choice of land-cover data, *Global Change Biol.*, 19(9), 2893–2906, doi:10.1111/gcb.12207.
- Ji, X. Y., G. B. Cui, L. Y. Yang, and Y. S. Wang (2006), Measurement of the CO<sub>2</sub> flux on the water-air interface of Taihu Lake, *J. Environ. Sci.*, 27(8), 1479–1486.
- Karim, A., J. Veizer, and J. Barth (2008), Net ecosystem production in the great lakes basin and its implications for the North American missing carbon sink: A hydrologic and stable isotope approach, *Global Planet. Change*, 61(1–2), 15–27, doi:10.1016/j.gloplacha.2007.08.004.
- Kicklighter, D. W., A. Bondeau, A. L. Schloss, J. Kaduk, A. D. McGuire, and P. P. N. M. Intercomparison (1999), Comparing global models of terrestrial net primary productivity (NPP): Global pattern and differentiation by major biomes, *Global Change Biol.*, 5, 16–24, doi:10.1046/j.1365-2486.1999.00003.x.
- Kirschbaum, M. U. F. (1995), The temperature-dependence Of soil organic-matter decomposition, and the effect of global warming on soil organic-C storage, *Soil Biol. Biochem.*, 27(6), 753–760, doi:10.1016/0038-0717(94)00242-5.
- Law, B. E., O. J. Sun, J. Campbell, S. Van Tuyl, and P. E. Thornton (2003), Changes in carbon storage and fluxes in a chronosequence of ponderosa pine, *Global Change Biol.*, 9(4), 510–524, doi:10.1046/j.1365-2486.2003.00624.x.
- Lee, X., et al. (2014), The Taihu Eddy Flux Network: An observational program on energy, water, And greenhouse gas fluxes of a large freshwater lake, *Bull. Am. Meteorol. Soc.*, 95(10), 1583–1594, doi:10.1175/Bams-D-13-00136.1.
- Li, Q., Z. H. Hu, H. X. Xue, Y. L. Wang, T. T. Tan, and D. L. Wu (2009), Variation of net ecosystem carbon flux over typical agro-ecosystem in Huaihe River basin [in Chinese], *J. Agro-Environ. Sci.*, 28(12), 2545–2550.
- Liu, J., J. M. Chen, J. Cihlar, and W. M. Park (1997), A process-based boreal ecosystem productivity simulator using remote sensing inputs, *Remote Sens. Environ.*, 62(2), 158–175, doi:10.1016/S0034-4257(97)00089-8.
- Liu, X. J., et al. (2013), Enhanced nitrogen deposition over China, *Nature*, 494(7438), 459–462, doi:10.1038/nature11917.
- Ma, S. X., G. Churkina, R. Wieland, and A. Gessler (2011), Optimization and evaluation of the ANTHRO-BGC model for winter crops in Europe, *Ecol. Modell.*, 222(20–22), 3662–3679, doi:10.1016/j.ecolmodel.2011.08.025.
- Ma, Y. C., X. W. Kong, B. Yang, X. L. Zhang, X. Y. Yan, J. C. Yang, and Z. Q. Xiong (2013), Net global warming potential and greenhouse gas intensity of annual rice-wheat rotations with integrated soil-crop system management, *Agric. Ecosyst. Environ.*, 164, 209–219, doi:10.1016/j.agee.2012.11.003.
- McGuire, A. D., et al. (2001), Carbon balance of the terrestrial biosphere in the twentieth century: Analyses of CO<sub>2</sub>, climate and land use effects with four process-based ecosystem models, *Global Biogeochem. Cycles*, 15(1), 183–206, doi:10.1029/2000GB001298.
- Melillo, J. M., A. D. McGuire, D. W. Kicklighter, B. Moore, C. J. Vorosmarty, and A. L. Schloss (1993), Global climate-change and terrestrial net primary production, *Nature*, 363(6426), 234–240, doi:10.1038/363234a0.
- Pan, G. X., L. S. Wu, L. Q. Li, X. H. Zhang, W. Gong, and Y. Wood (2008), Organic carbon stratification and size distribution of three typical paddy soils from Taihu Lake region, China, *J. Environ. Sci.*, 20(4), 456–463, doi:10.1016/S1001-0742(08)62079-3.
- Parton, W. J., et al. (1993), Observations and modeling of biomass and soil organic-matter dynamics for the Grassland biome worldwide, *Global Biogeochem. Cycles*, 7(4), 785–809, doi:10.1029/93GB02042.
- Petritsch, R., H. Hasenauer, and S. A. Pietsch (2007), Incorporating forest growth response to thinning within BIOME-BGC, *For. Ecol. Manage.*, 242(2–3), 324–336, doi:10.1016/j.foreco.2007.01.050.
- Potter, C. S., J. T. Randerson, C. B. Field, P. A. Matson, P. M. Vitousek, H. A. Mooney, and S. A. Klooster (1993), Terrestrial ecosystem production —A process model-based on global satellite and surface data, *Global Biogeochem. Cycles*, 7(4), 811–841, doi:10.1029/93GB02725.
- Robinson, D. T., D. G. Brown, and W. S. Currie (2009), Modelling carbon storage in highly fragmented and human-dominated landscapes: Linking land-cover patterns and ecosystem models, *Ecol. Modell.*, 220(9–10), 1325–1338, doi:10.1016/j.ecolmodel.2009.02.020.
- Robinson, D. T., S. P. Sun, M. Hutchins, R. L. Riolo, D. G. Brown, D. C. Parker, T. Filatova, W. S. Currie, and S. Kiger (2013), Effects of land markets and land management on ecosystem function: A framework for modelling exurban land-change, *Environ. Model. Software*, 45, 129–140, doi:10.1016/j.envsoft.2012.06.016.
- Running, S. W., and R. E. Hunt (1993), Generalization of a forest ecosystem process model for other biomes, BIOME-BGC, and an application for global-scale models, in *Scaling Physiological Processes: Leaf to Globe*, edited by J. R. Ehleringer and C. B. Field, pp. 145–157, Academic Press, San Diego, Calif.
- The State Council of the People's Republic of China (2014), *National New-Type Urbanization Plan 2014–2020 (in Chinese)*, People's Publishing House, Beijing, China.
- Schimel, D. S., et al. (2001), Recent patterns and mechanisms of carbon exchange by terrestrial ecosystems, *Nature*, 414(6860), 169–172, doi:10.1038/35102500.
- Schulp, C. J. E., G. J. Nabuurs, and P. H. Verburg (2008), Future carbon sequestration in Europe—Effects of land use change, *Agric. Ecosyst. Environ.*, 127(3–4), 251–264, doi:10.1016/j.agee.2008.04.010.

- Shi, Y. (2013), Vegetation structure characteristics and carbon uptake of urban built-up area in China [in Chinese], Doctor thesis, Zhejiang Univ., Hangzhou, China.
- Tang, X. G., Z. Ding, H. P. Li, X. Y. Li, J. H. Luo, J. Xie, and D. Q. Chen (2015a), Characterizing ecosystem water-use efficiency of croplands with eddy covariance measurements and MODIS products, *Ecol. Eng.*, *85*, 212–217, doi:10.1016/j.ecoleng.2015.09.078.
- Tang, X. G., H. P. Li, N. Huang, X. Y. Li, X. B. Xu, Z. Ding, and J. Xie (2015b), A comprehensive assessment of MODIS-derived GPP for forest ecosystems using the site-level FLUXNET database, *Environ. Earth Sci.*, *74*(7), 5907–5918, doi:10.1007/s12665-015-4615-0.
- Tatarinov, F. A., E. Cienciala, P. Vopenka, and V. Avilov (2011), Effect of climate change and nitrogen deposition on central-European forests: Regional-scale simulation for South Bohemia, *For. Ecol. Manage.*, *262*(10), 1919–1927, doi:10.1016/j.foreco.2011.02.020.
- Thornton, P. E., et al. (2002), Modeling and measuring the effects of disturbance history and climate on carbon and water budgets in evergreen needleleaf forests, *Agric. For. Meteorol.*, *113*(1–4), 185–222.
- Tomáš, H., B. Zoltán, B. Ivan, M. Katarína, S. Róbert, K. Anikó, P. Jozef, B. Borbála, F. Marek, and C. Galina (2014), Future carbon cycle in mountain spruce forests of central Europe: Modelling framework and ecological inferences, *For. Ecol. Manage.*, *328*, 55–68.
- Trusilova, K. T., J. Trembath, and G. Churkina (2009), Parameter estimation and validation of the terrestrial ecosystem model BIOME-BGC using eddy-covariance flux measurements, Rep, Technical reports Max-Planck-Institut für Biogeochemie 16, Germany.
- Ueyama, M., et al. (2010), Simulating carbon and water cycles of larch forests in East Asia by the BIOME-BGC model with AsiaFlux data, *Biogeosciences*, *7*(3), 959–977.
- Wang, Q. X., W. Masataka, and O. Y. Zhu (2005), Simulation of water and carbon fluxes using BIOME-BGC model over crops in China, *Agric. For. Meteorol.*, *131*(3–4), 209–224, doi:10.1016/j.agrformet.2005.06.002.
- Wang, W., K. Ichii, H. Hashimoto, A. R. Michaelis, P. E. Thornton, B. E. Law, and R. R. Nemani (2009), A hierarchical analysis of terrestrial ecosystem model BIOME-BGC: Equilibrium analysis and model calibration, *Ecol. Modell.*, *220*(17), 2009–2023, doi:10.1016/j.ecolmodel.2009.04.051.
- Ward, H. C., S. Kotthaus, C. S. B. Grimmond, A. Björkegren, M. Wilkinson, W. T. J. Morrison, J. G. Evans, J. I. L. Morison, and M. Iamarino (2015), Effects of urban density on carbon dioxide exchanges: Observations of dense urban, suburban and woodland areas of southern England, *Environ. Pollut.*, *198*, 186–200, doi:10.1016/j.envpol.2014.12.031.
- Weissert, L. F., J. A. Salmond, and L. Schwendenmann (2014), A review of the current progress in quantifying the potential of urban forests to mitigate urban CO<sub>2</sub> emissions, *Urban Clim.*, *8*, 100–125.
- White, M. A., P. E. Thornton, S. W. Running, and R. R. Nemani (2000), Parameterization and sensitivity analysis of the BIOME-BGC terrestrial ecosystem model: Net primary production controls, *Earth Interact.*, *4*, 1–85, doi:10.1175/1087-3562(2000)004<0003:PASAOT>2.0.CO;2.
- Wu, C. Y., J. M. Chen, A. Gonsamo, D. T. Price, T. A. Black, and W. A. Kurz (2012), Interannual variability of net carbon exchange is related to the lag between the end-dates of net carbon uptake and photosynthesis: Evidence from long records at two contrasting forest stands, *Agric. For. Meteorol.*, *164*, 29–38, doi:10.1016/j.agrformet.2012.05.002.
- Wu, S. H., S. L. Zhou, D. X. Chen, Z. Q. Wei, L. Dai, and X. G. Li (2014), Determining the contributions of urbanisation and climate change to NPP variations over the last decade in the Yangtze River delta, China, *Sci. Total Environ.*, *472*, 397–406.
- Xing, Y. P., P. Xie, H. Yang, L. Y. Ni, Y. S. Wang, and K. W. Rong (2005), Methane and carbon dioxide fluxes from a shallow hypereutrophic subtropical Lake in China, *Atmos. Environ.*, *39*(30), 5532–5540, doi:10.1016/j.atmosenv.2005.06.010.
- Xinhuanet (2013), President Xi vows strict observation of ecological “red line”, Beijing.
- Xu, X. B., G. S. Yang, and H. P. Li (2011), Impacts of land use change on net primary productivity in the Taihu Basin, China [in Chinese], *Res. Sci.*, *33*, 1940–1947.
- Xu, X. B., G. S. Yang, and X. X. Sun (2015), Analysis of net ecosystem CO<sub>2</sub> exchange (NEE) in the rice-wheat rotation agroecosystem of the Lake Taihu Basin, China [in Chinese], *Acta Ecol. Sin.*, *35*(20), 6655–6665.
- Xu, X. B., G. S. Yang, Y. Tan, Q. L. Zhuang, H. P. Li, R. R. Wan, W. Z. Su, and J. Zhang (2016), Ecological risk assessment of ecosystem services in the Taihu Lake Basin of China from 1985 to 2020, *Sci. Total Environ.*, *554*–555, 7–16.
- Zhang, X. X., S. Yin, Y. S. Li, H. L. Zhuang, C. S. Li, and C. J. Liu (2014), Comparison of greenhouse gas emissions from rice paddy fields under different nitrogen fertilization loads in Chongming Island, Eastern China, *Sci. Total Environ.*, *472*, 381–388, doi:10.1016/j.scitotenv.2013.11.014.
- Zhao, M., Z. H. Kong, F. J. Escobedo, and J. Gao (2010), Impacts of urban forests on offsetting carbon emissions from industrial energy use in Hangzhou, China, *J. Environ. Manage.*, *91*(4), 807–813, doi:10.1016/j.jenvman.2009.10.010.
- Zhou, B. Z. (2006), Dynamics of bamboo’s below-ground system based on minirhizotron technique (in Chinese), PhD dissertation thesis, Chinese Academy of Forestry, Beijing.
- Zhou, G. M. (2006), Carbon storage, fixation and distribution in mao bamboo (*Phyllostachys pubescens*) stands ecosystem (in Chinese), PhD dissertation thesis, Zhejiang Univ., Hanzhou, China.
- Zhu, Q., and Q. L. Zhuang (2014), Parameterization and sensitivity analysis of a process-based terrestrial ecosystem model using adjoint method, *J. Adv. Model. Earth Syst.*, *6*(2), 315–331, doi:10.1002/2013MS000241.